

## XANES and EXAFS measurements of plutonium hydrates

T. Reich, G. Geipel, H. Funke, C. Hennig, A. Roßberg, G. Bernhard  
Institute of Radiochemistry, Forschungszentrum Rossendorf, P.O.B. 510119, 01314 Dresden,  
Germany

### 1. Introduction

This report describes the first X-ray Absorption Fine-Structure (XAFS) measurement of plutonium samples at ROBL. Two liquid samples containing Pu(III) and Pu(VI) hydrates were chosen for this experiment. The goal of this study was twofold. Firstly, we wanted to demonstrate that all requirements were met for the preparation and transportation of plutonium solutions from the home institution in Germany to the ESRF and for the XAFS measurements at ROBL. This should encourage others to do similar experiments on transuranium samples. Secondly, the hydrate is the simplest chemical form of plutonium in solution. The knowledge of the structural parameters of the hydration sphere is important for the interpretation of Extended X-ray Absorption Fine-Structure (EXAFS) results on complicated aqueous plutonium complexes or sorbates on mineral surfaces where the water molecules are partly or fully replaced by other ligands. In general, the number of water molecules in the hydration sphere depends on such factors as ionic radius and charge and ionic strength. The aquo ions of trivalent actinides have the general formula  $An(H_2O)_n^{3+}$ . In the literature the number of water molecules in the hydration sphere is discussed controversially and values range from eight to eleven [1]. It has been established that hexavalent actinides form trans-dioxo cations,  $AnO_2(H_2O)_n^{2+}$ , with five water molecules in the hydration sphere.

### 2. Experimental

High-purity  $PuO_2$  (Pu-242) purchased from AEA Technology, QSA GmbH served as starting material for the sample preparation. It was dissolved by catalytic oxidation to Pu(VI) according to the following reaction:  $2Ag^{2+} + PuO_2 = PuO_2^{2+} + 2Ag^+$ . The silver ions were removed from the reaction solution by electrochemical reduction to  $Ag^0$ . Part of the Pu(VI) solution was electrochemically reduced to Pu(III). The Pu(III) and Pu(VI) hydrates were in perchloric and nitric media (1 M acidic solution), respectively. The final Pu concentration was 50 mM. The Pu oxidation states were confirmed by UV/Vis measurements [2]. For the XAFS measurements, 4.7 mL solution was filled and sealed in polyethylene cuvettes of 10 mm path length. The samples were measured at ROBL within 48 hours after their preparation in Rossendorf.

Three scans of the Pu  $L_{III}$ -edge (18057 eV) and  $L_I$ -edge (23104 eV) XAFS spectra were collected in transmission mode at room temperature using the Si(111) double-crystal monochromator in fixed-exit mode [3]. For energy calibration purpose, the transmission spectra of metallic reference foils were measured simultaneously with the sample. The Pu  $L_{III}$ -edge XAFS spectrum was calibrated using the first inflection point of the K-edge absorption spectrum of a Zr foil (17997 eV). The K-edge absorption spectrum of a Pd foil (24354 eV) was measured to calibrate the Pu  $L_I$ -edge XAFS spectrum. The energy shifts relative to these references was less than 0.5 eV during the entire measurement.

The EXAFSPAK software package [4] was used for the EXAFS analysis. Theoretical scattering phases and amplitudes for the Pu  $L_{III}$ -edge EXAFS analysis were calculated for

hypothetical clusters of  $\text{PuO}_8$  and  $\text{PuO}_2\text{O}_5$  using FEFF6 [5]. For the cubic  $\text{PuO}_8$  cluster, the assumed Pu-O bond distance was 2.39 Å. The Pu-O bond distances in the pentagonal bipyramid  $\text{PuO}_2\text{O}_5$  were 1.76 and 2.41 Å, respectively. In addition to the Pu-O single-scattering paths, the multiple-scattering (MS) path  $\text{Pu} \rightarrow \text{O}_1 \rightarrow \text{Pu} \rightarrow \text{O}_2 \rightarrow \text{Pu}$  within the linear O-Pu-O chain was calculated. This MS path was included in the EXAFS fit of the Pu(VI) hydrate in a similar way as described for uranyl compounds [6]. The amplitude reduction factor,  $S_0^2$ , equalled 0.9. The shift in threshold energy,  $\Delta E_0$ , was varied as one global fit parameter for all scattering paths.

### 3. Results and Discussion

#### 3.1 Pu XANES Spectra

The Pu  $L_{\text{III}}$ -edge X-ray Absorption Near-Edge Structure (XANES) of Pu(III) and Pu(VI) hydrates are shown in Fig. 1. Both spectra were normalised to equal intensity at 18200 eV.

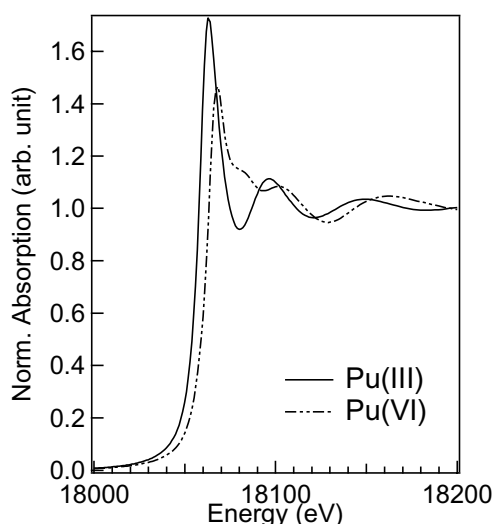


**Fig. 1:** Experimental  $L_{\text{III}}$ -edge XANES spectra of Pu hydrates.

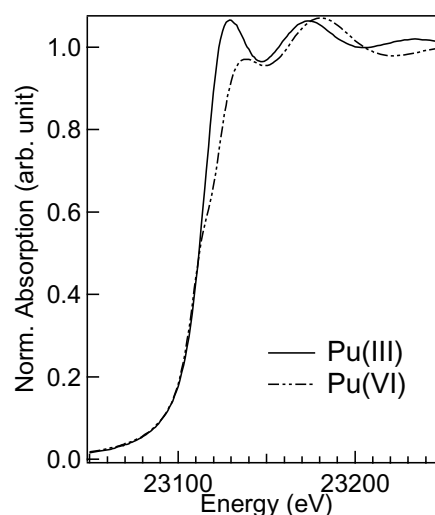


**Fig. 2:** Experimental  $L_{\text{I}}$ -edge XANES spectra of Pu hydrates.

The inflection point of the rising edge of the XANES spectra has been determined and is used throughout this paper as the energy position of the absorption edge. The  $L_{\text{III}}$ -edge energy of the Pu(III) and Pu(VI) hydrates is 18058.1 and 18062.3 eV, respectively (Tab. 1). The 4 eV shift of the  $L_{\text{III}}$  absorption edge of Pu(VI) toward higher energy as compared to Pu(III) can also be seen in Fig. 1. The distinct differences in the XANES features of Pu hydrates have been reproduced by *ab initio* calculations with the code FEFF7 [7]. However, there are quantitative discrepancies in the theoretical edge positions for the different Pu oxidation states. The experimental values of the Pu  $L_{\text{III}}$ -edge energies for tri-, tetra-, penta-, and hexavalent Pu aquo ions are 18060.1, 18063.2, 18062.6, and 18064.8 eV, respectively [8]. These values for trivalent and hexavalent Pu agree with our result after taking into account a 2 eV difference in the energy of Zr K-edge, which was used for energy calibration. When using the simple method of defining the edge energy as the first inflection point, it is difficult or impossible to derive the Pu oxidation state from it, in particular for mixtures of the oxidation states (IV)/(V), (IV)/(VI), and (V)/(VI).

The XANES at the Pu  $L_{\text{I}}$ -edge (Fig. 2) differs significantly from the  $L_{\text{III}}$ -edge spectra due to the dipole selection rule and the density of unoccupied states. The optical transition at the  $L_{\text{I}}$  and  $L_{\text{III}}$  edges, respectively, mainly map the unoccupied 7p and 6d states in the presence of

**Table 1:** Experimental Pu L<sub>III</sub>- and L<sub>I</sub>-edge energies of Pu(III) and Pu(VI) hydrates derived from the inflection point of the XANES spectrum.

Edge	Edge energy (eV)		$\Delta E$ (eV)
	Pu(III)	Pu(VI)	
Pu L <sub>III</sub>	18058.1	18062.3	4.2
Pu L <sub>I</sub>	23115.4	23109.0	-6.4
		23123.5	8.1

The energy axis was calibrated using the K-edges at 17997 and 24354 eV from Zr and Pd foils, respectively.

the core hole. For the Pu(III) hydrate, the L<sub>I</sub> absorption edge has one inflection point at 23115.4 eV (Tab. 1). In contrast, two inflection points at 23109.0 and 23123.5 eV are observed for the L<sub>I</sub> absorption edge of Pu(VI) hydrate. It should be noted that this splitting of 14 eV could not be reproduced by *ab initio* calculations using FEFF7. Only a single inflection point is seen in the XANES calculation of Pu hydrates [7]. It may be necessary in this case to use *ab initio* molecular orbital methods to obtain a better agreement between theoretical and experimental L<sub>I</sub>-edge XANES features of Pu(VI) hydrate. It appears that the L<sub>I</sub>-edge XANES is more sensitive to changes in the electronic and molecular structure of Pu species and, therefore, more suited for oxidation state determination using XANES than the L<sub>III</sub> edge.

### 3.2 Pu EXAFS Spectra

The different molecular structures of Pu(III) and Pu(VI) hydrates are also reflected in the EXAFS spectra shown in Fig. 3. The Pu L<sub>III</sub>-edge k<sup>3</sup>-weighted EXAFS spectrum of Pu(III) hydrate shows a single-frequency oscillation and the corresponding Fourier transform (FT)

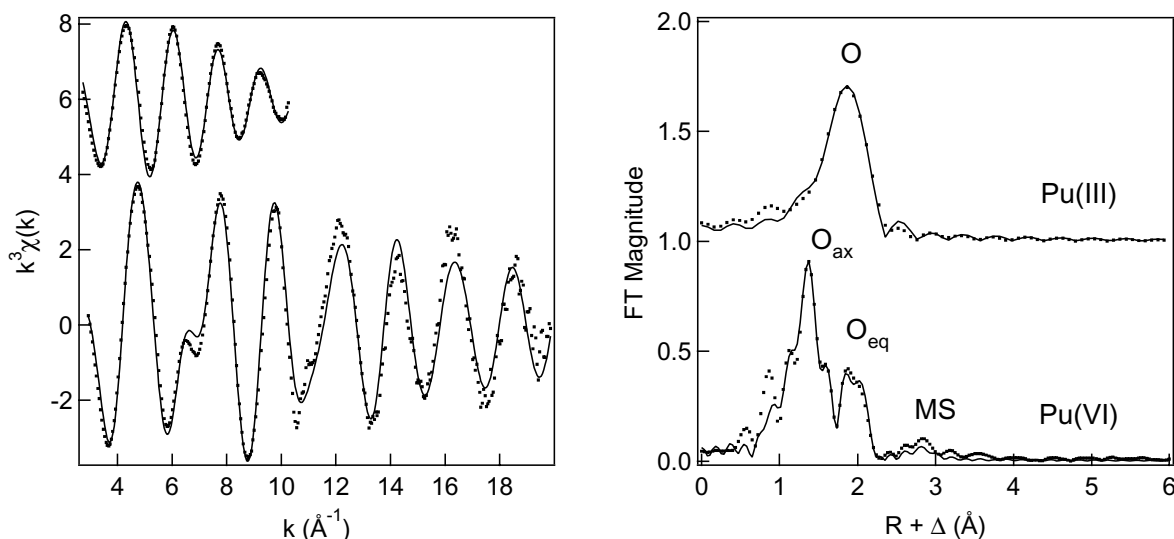


**Fig. 3:** Raw Pu L<sub>III</sub>-edge k<sup>3</sup>-weighted EXAFS data (left) and corresponding Fourier transforms (right) for Pu hydrates: experimental data - dotted line; theoretical fit - solid line.

only one peak. Therefore, the experimental EXAFS spectrum was modelled with one Pu-O coordination shell. The obtained structural parameters are summarised in Tab. 2. The hydration sphere of Pu(III) consists of approximately eight water molecules with an average Pu-O distance of 2.48 Å. These results can be compared to those of an EXAFS study of a 20 mM Pu(III) solution in 10 mM LiCl [9] (see Tab. 2). The Pu L<sub>III</sub>-edge k<sup>3</sup>-weighted EXAFS

spectrum was analysed using the same software, i.e., EXAFSPAK and FEFF6. According to this study, the Pu(III) aquo ion coordinates approximately ten water molecules at a Pu-O distances of 2.51 Å. In a later publication by the same group [10], their previous Pu L<sub>III</sub>-edge EXAFS spectrum was fit with  $S_0^2$  set equal to 1.0 instead of 0.9. As a result, the Pu-O coordination number decreased from 10.2. to 9.2 (Tab. 2). The Pu-O bond distance remained unchanged. It should be noted that partly due to the uncertainties of the correct choice of the parameter  $S_0^2$ , the accuracy in the determination of coordination numbers from EXAFS is  $\pm 1$  [11]. Differences between these results and our result may indicate an influence of the media (10 mM LiCl vs. 1 M HClO<sub>4</sub>) on the hydration sphere of Pu(III). This effect should be studied in more detail to verify its nature. EXAFS structural parameters of Pu(III) aquo ions are also given in refs. [12, 13]. The coordination numbers are between eight and ten. The Pu-O bond distances range from 2.49 to 2.51 Å (Tab. 2). Unfortunately, these authors gave non or very little experimental details on their EXAFS experiments.

The Pu L<sub>III</sub>-edge  $k^3$ -weighted EXAFS spectrum of Pu(VI) hydrate shows two oscillations (Fig. 3). Therefore, the corresponding FT shows two peaks due to the axial, O<sub>ax</sub>, and equatorial, O<sub>eq</sub>, oxygen atoms, respectively. The weak feature in the FT at  $R+\Delta \approx 2.8$  Å is the MS contribution of the plutonyl moiety. The theoretical model to fit the experimental data

**Table 2:** EXAFS structural parameters for Pu(III) hydrates.

[Pu] mM	Medium	R(Å)	N	$\sigma^2(\text{Å}^2)$	Ref.
50	1 M HClO <sub>4</sub>	2.48	7.6(2) <sup>a</sup>	0.010	Present
20	0.01 M LiCl	2.51	10.2(2) <sup>a</sup>	0.010	[9]
20	0.01 M LiCl	2.51	9.2(3) <sup>a</sup>	0.010	[10]
-	-	2.49	8-9		[12]
-	1 M HCl, Zn amalgam	2.51(1) <sup>a</sup>	9.9(9) <sup>a</sup>	0.010(2) <sup>a</sup>	[13]

<sup>a</sup> The 95% confidence limit is given in parentheses. The errors in R and  $\sigma^2$  are estimated as  $\pm 0.01$  Å and  $\pm 0.001$  Å<sup>2</sup>, respectively.

included two single-scattering paths O<sub>ax</sub> and O<sub>eq</sub> and the MS path. The Pu-O<sub>ax</sub> distance in the plutonyl group is 1.74 Å (Tab. 3). In the equatorial plane, the Pu is coordinated by four to five water molecules with a Pu-O<sub>eq</sub> distance of 2.42 Å. As to our knowledge, this result can be compared only with the result of ref. [12] (Tab. 3). Within the experimental uncertainties the results are in good agreement except for the O<sub>eq</sub> coordination number (Tab. 3). Given the lack of experimental information, one cannot discuss the difference in the O<sub>eq</sub> coordination number, i.e., 4.4 vs. 6.

**Table 3:** EXAFS structural parameters for Pu(VI) hydrates.

[Pu] mM	Medium	Shell	R(Å)	N	$\sigma^2(\text{Å}^2)$	Ref.
50	1 M HNO <sub>3</sub>	O <sub>ax</sub>	1.74	1.9(1) <sup>a</sup>	0.001	Present
		O <sub>eq</sub>	2.42	4.4(2) <sup>a</sup>	0.005	
-	-	O <sub>ax</sub>	1.74	2		[12]
		O <sub>eq</sub>	2.40	6		

<sup>a</sup> The 95% confidence limit is given in parentheses. The errors in R and  $\sigma^2$  are estimated as  $\pm 0.01$  Å and  $\pm 0.001$  Å<sup>2</sup>, respectively.

Table 4 compares the EXAFS structural parameters of hexavalent U, Np [14], and Pu hydrates measured at ROBL. As one can see, the structural parameters both for the axial and the equatorial oxygen coordination shell are almost identical. However, two weak dependencies are seen. Firstly, the An-O<sub>ax</sub> bond distance decreases from 1.76 to 1.74 Å by

going from U to Pu. This is in agreement with the well-known actinide contraction [15]. Secondly, the  $O_{eq}$  coordination number determined by EXAFS decreases systematically from 4.9 to 4.4 from U to Pu. The average An- $O_{eq}$  bond length remains unchanged. Again, due to the relatively large error in the determination of coordination numbers, it is difficult to draw conclusions from this small decrease without further systematic EXAFS studies, in combination with other spectroscopic techniques, over a range of different sample conditions.

**Table 4:**

EXAFS structural parameters for An(VI) hydrates. The An concentration was 50 mM.

An	Medium	Shell	R(Å)	N <sup>a</sup>	$\sigma^2(\text{Å}^2)$	Ref.
U	1 M HClO <sub>4</sub>	O <sub>ax</sub>	1.76	1.9(1)	0.001	Present
		O <sub>eq</sub>	2.41	4.9(2)	0.006	
Np	0.1 M HNO <sub>3</sub>	O <sub>ax</sub>	1.75	2.0(1)	0.002	[14]
		O <sub>eq</sub>	2.41	4.6(2)	0.006	
Pu	1 M HNO <sub>3</sub>	O <sub>ax</sub>	1.74	1.9(1)	0.001	Present
		O <sub>eq</sub>	2.42	4.4(2)	0.005	

<sup>a</sup> The 95% confidence limit is given in parentheses. The errors in R and  $\sigma^2$  are estimated as  $\pm 0.01$  Å and  $\pm 0.001$  Å<sup>2</sup>, respectively.

#### 4. Conclusion

In summary, the first XAFS measurements of aqueous solutions of Pu-242 were an important milestone for the Rossendorf Beamline ROBL. The Pu L<sub>III</sub>- and L<sub>I</sub>-edge XANES spectra of Pu(III) and Pu(VI) are sensitive to changes in the electronic and molecular structures of the Pu species and can be used for the identification of these Pu oxidation states. In case of environmental samples, which may contain several Pu oxidation states simultaneously, it is recommended to utilise the Pu L<sub>I</sub>-edge XANES for the determination of Pu oxidation states.

The Pu(III) aquo ion can be written as Pu(H<sub>2</sub>O)<sub>8</sub><sup>3+</sup> with an average Pu-O bond distance of 2.48 Å. The Pu(VI) forms a plutonyl ion PuO<sub>2</sub>(H<sub>2</sub>O)<sub>4-5</sub><sup>2+</sup>. The axial and equatorial Pu-O bond distances are 1.74 and 2.42 Å. Future studies on these species should determine the influence of Pu concentration and the conditions of the media (ionic strength, electrolyte) on the hydration sphere. These studies will also include the *in situ* preparation of Pu oxidation states, which are not stable during transportation from the home institute to ROBL. Recently, all oxidation states from Np(III) to Np(VII) have been prepared in a spectroelectrochemical cell [16], which was positioned in the synchrotron beam at the Advanced Photon Source to simultaneously record the Np L<sub>III</sub>-edge XANES [17] and EXAFS spectra [18]. The knowledge of the EXAFS structural parameters of the Pu hydrates are important for the interpretation of EXAFS results on complicated systems. In so far, such measurements contribute toward a better understanding of the behaviour of actinide elements in the environment.

#### Acknowledgement

We thank G. Grambole for her help during the sample preparation.

#### References

- [1] Madic, C., Den Auwer, C. and Guillaumont, R., Application of X-ray absorption spectroscopy (XAS) to actinide solution chemistry, Euroconference and NEA Workshop on Speciation,

- Techniques, and Facilities for Radioactive Materials at Synchrotron Light Sources (NEA/OECD (Paris), Grenoble, France, 1999), pp. 69-79.
- [2] Weigel, F., Kratz, J.J. and Seaborg, G.T., in: *The chemistry of the actinide elements*, Eds. J. J. Kratz, G.T. Seaborg, L.R. Morss (Chapman & Hall, London New York, 1986), vol. 1, pp. 582-587.
- [3] Matz, W., Schell, N., Bernhard, G., Prokert, F., Reich, T., Claußner, J., Oehme, W., Schlenk, R., Diemel, S., Funke, H., Eichhorn, F., Betzl, M., Pröhl, D., Strauch, U., Hüttig, G., Krug, H., Neumann, W., Brendler, V., Reichel, P., Denecke, M.A. and Nitsche, H., ROBL - a CRG beamline for radiochemistry and materials research at the ESRF, *J. Synchrotron Rad.* **6** (1999) 1076-1085.
- [4] George, G.N. and Pickering, I.J., Stanford Synchrotron Radiation Laboratory, EXAFSPAK: A Suite of Computer Programs for Analysis of X-Ray Absorption Spectra (1995).
- [5] Zabinsky, S.I., Rehr, J.J., Ankudinov, A., Albers, R.C. and Eller, M.J., Multiple-scattering calculations of x-ray-absorption spectra, *Phys. Rev. B* **52** (1995) 2995-3009.
- [6] Hudson, E.A., Allen, P.G., Terminello, L.J., Denecke, M.A. and Reich, T., Polarized x-ray-absorption spectroscopy of the uranyl ion: Comparison of experiment and theory, *Phys. Rev. B* **54** (1996) 156-165.
- [7] Ankudinov, A.L., Conradson, S.D., Mustre de Leon, J. and Rehr, J.J., Relativistic XANES calculations of Pu hydrates, *Phys. Rev. B* **57** (1998) 7518-7525.
- [8] Conradson, S.D., Al Mahamid, I., Clark, D.L., Hess, N.J., Hudson, E.A., Neu, M.P., Palmer, P.D., Runde, W.H. and Tait, C.D., Oxidation state determination of plutonium aquo ions using x-ray absorption spectroscopy, *Polyhedron* **17** (1998) 599-602.
- [9] Allen, P.G., Bucher, J.J., Shuh, D.K., Edelstein, N.M. and Reich, T., Investigation of aquo and chloro complexes of  $\text{UO}_2^{2+}$ ,  $\text{NpO}_2^+$ ,  $\text{Np}^{4+}$ , and  $\text{Pu}^{3+}$  by X-ray absorption fine structure spectroscopy, *Inorg. Chem.* **36** (1997) 4676-4683.
- [10] Allen, P.G., Bucher, J.J., Shuh, D.K., Edelstein, N.M. and Craig, I., Coordination chemistry of trivalent lanthanide and actinide ions in dilute and concentrated chloride solutions, *Inorg. Chem.* **39** (2000) 595-601.
- [11] Rehr, J.J. and Ankudinov, A.L., New developments in the theory of X-ray absorption and core photoemission, *J. Electron Spectrosc. Related Phenom.* **114-116** (2001) 1115-1121.
- [12] Conradson, S.D., Application of X-ray absorption fine structure spectroscopy to materials and environmental science, *Appl. Spectrosc.* **52** (1998) 252A-279A.
- [13] David, F., Fourest, B., Hubert, S., Le Du, J.F., Revel, R., Den Auwer, C., Madic, C., Morss, L.R., Ionova, G., Mikhalko, V., Vokhmin, V., Nikonov, M., Berthlet, J.C. and Ephritikhine, M., Aquo ions of some trivalent actinides: EXAFS data and thermodynamic consequences, Euroconference and NEA Workshop on Speciation, Techniques, and Facilities for Radioactive Materials at Synchrotron Light Sources (NEA/OECD (Paris), Grenoble, France, 1999), pp. 95-100.
- [14] Reich, T., Bernhard, G., Geipel, G., Funke, H., Hennig, C., Rossberg, A., Matz, W., Schell, N. and Nitsche, H., The Rossendorf Beam Line ROBL - a dedicated experimental station for XAFS measurements of actinides and other radionuclides, *Radiochim. Acta* **88** (2000) 633-637.
- [15] Kratz, J.J., Morss, L.R. and Seaborg, G.T., in: *The chemistry of the actinide elements*, Eds. J. J. Kratz, G. T. Seaborg, L. R. Morss (Chapman and Hall, London New York, 1986), vol. 2, pp. 1164-1165.
- [16] Antonio, M.R., Soderholm, L. and Song, I., Design of spectroelectrochemical cell for in situ X-ray absorption fine structure measurements of bulk solution species, *J. Appl. Electrochem.* **27** (1997) 784-792.
- [17] Soderholm, L., Antonio, M.R., Williams, C. and Wasserman, S.R., XANES spectroelectrochemistry: A new method for determining formal potentials, *Anal. Chem.* **71** (1999) 4622-4628.
- [18] Antonio, R., Soderholm, L., Williams, C.W., Blaudeau, J.P. and Bursten, B.E., Neptunium redox speciation, *Radiochim. Acta* **89** (2001) 17-26.